ELSEVIER

Thermochimica Acta 337 (1999) 163–168

thermochimica acta

www.elsevier.com/locate/tca

Characteristic length of glass transition from calorimetry for benzoin isobutylether in a series of nanometer pores

E. Hempel[a], A. Huwe[b], K. Otto[c], F. Janowski[c], K. Schröter[a], E. Donth[a,*]

[a]*Fachbereich Physik, Universität Halle, D-06099 Halle Saale, Germany*
[b]*Fakultät für Physik, Universität Leipzig, D-04103 Leipzig, Germany*
[c]*Fachbereich Chemie, Universität Halle, D-06099 Halle Saale, Germany*

Received 14 May 1999; accepted 31 May 1999

Abstract

Temperature modulated dynamic scanning calorimetry (TMDSC) yields the characteristic length or, correspondingly, the cooperativity of dynamic glass transition of a molecular liquid in nanometer size pores. The TMDSC traces for benzoin isobutylether are not disturbed by structuring effects that are usually observed in standard DSC. The bulk length of about $\xi_\alpha = 3$ nm decreases with decreasing pore diameter below $D = 12$ nm, down to $\xi_\alpha = 1.6$ nm in $D = 2$ nm pores. The glass transition temperature decreases concomitantly. This can be understood in the framework of the hindered glass transition.

Keywords: Glass transition; Calorimetry

1. Introduction

There is growing evidence that the dynamic glass transition is related to a dynamic heterogeneity [1]. Sophisticated experiments try to select sub-ensembles of different mobility [2,3]. A relation of dynamic heterogeneity to a corresponding spatial length scale seems natural. Such a 'characteristic length' ξ_α [4] may be identified with the average size of cooperatively rearranging regions CRR as introduced by Adam and Gibbs [5]. A CRR is defined as a subsystem which, upon a sufficient thermodynamic fluctuation, can rearrange into another configuration independently of its environment. NMR [3] and calorimetry [4] find a consistent characteristic length of $\xi_\alpha = 3$ nm for poly(vinyl acetate).

Scattering experiments so far did not find any indication of this length scale in the nm-range [6]. Responsible for the scattering contrast are density fluctuations. Because ξ_α is related to the free volume at the glass transition only very small scattering effects are to be expected.

Another way to identify the responsible length scale are experiments on glass formers in confining geometries. Dielectric experiments on molecular liquids in porous glasses [7,8] and droplets [8] show a decrease of the dynamic glass transition temperature (increasing α relaxation frequency) with confinement.

In an idealized picture one would expect no influence of confinement as long as the responsible length

*Corresponding author. Fax: +49-0345-5527017
E-mail address: donth@physik.uni-halle.de (E. Donth)

0040-6031/99/$ – see front matter
PII: S0040-6031(99)00168-9

scale is greater than the characteristic length of cooperativity. Just if they coincide a change in relaxation properties should occur. In practice the influence of the confining walls on the mobility of molecules already starts at greater length scales. Lubricated surfaces are used to prevent the liquid from chemical bonds with the inner pore surface [7,9]. Even then some geometrical effect of the nearby surface on the mobility of the liquid molecules remains [10]. The same holds for experiments on the mobile amorphous phase of partially crystalline polymers. This phase is confined between rigid amorphous surface layers of crystalline lamella. Such experiments have the advantage that mobile phase and confinement are of the same chemical composition, and interactions are expected to be small [11].

The CRR is defined by statistical independence which leads directly [12,13] to a calorimetric fluctuation formula for the average CRR size:

$$\xi_\alpha^3 = k_B T^2 \Delta(1/c_v)/\rho\delta T^2 \approx k_B T^2 \Delta c_p/\bar{c}_p^2 \rho\delta T^2, \quad (1)$$

where all important variables on the right-hand side can approximately be determined from temperature modulated DSC (TMDSC) [13]. In Eq. (1), ξ_α is the size of a CRR, $V_\alpha = \xi_\alpha^3$, ρ the mass density, k_B the Boltzmann constant, $\Delta(1/c_v)$ the step height of the reciprocal specific heat at constant volume (approximated by $\Delta c_p/\bar{c}_p^2$ in this work), and δT^2 the *ms* temperature fluctuation related to the dynamic glass transition of one CRR [12–14]. In this paper, δT is determined as the dispersion of a Gaussian fit for the imaginary part of isochronous dynamic heat capacity [15],

$$c_p''(T) \sim \exp[(T - T_{max})^2/2\delta T^2]. \quad (2)$$

The proof, for Gaussian distributions in the framework of linear response, that this dispersion δT is identical to the temperature fluctuation of a CRR will be published elsewhere [16].

The characteristic length is typically $\xi_\alpha \approx 2$–3 nm [4] at the glass temperature, T_g, for substances where T_g is far below the crossover temperature. The corresponding volume contains a particle number of order 100. Such experiments were done so far on bulk substances. In this paper calorimetric experiments on the molecular liquid benzoin isobutylether (BIBE) confined in porous glasses of different pore diameter are presented.

The BIBE liquid was selected because it has only a weak tendency to crystallization and water absorption. Dielectric and dynamic calorimetric data of the bulk liquid are available [17].

The aim of this paper is to find a correlation between the calorimetrically estimated length ξ_α and the pore diameter D to obtain an independent argument for the existence and size of the characteristic length of glass transition.

2. Experimental

2.1. Sample

The sample was purchased from Aldrich. BIBE is a photo initiator. It was purified by distillation under reduced pressure over a short column (bp(2 mbar) = 154°C).

The porous glasses with pore diameters of 7.5, 5, and 2.5 nm are commercial products (GelTech). They are produced by a sol–gel-technique. Additionally one glass with a pore diameter of 2 nm was prepared by spinodal decomposition. This yields glasses with a narrower distribution of pore diameters and a slightly different geometry (more sphere-like compared to more tube-like for sol–gel glasses) [18,19].

All porous glasses were silanisized. Two different lubricants were used. For series I dimethyl aminotriethyl silane was used. The pores of series II were coated with dimethyl hexamethyl disilane. The ethyl groups of series I should better cover the surface. Treatment of samples prior to loading with BIBE and pore filling are described in [7].

2.2. DSC and TMDSC

A DSC 7 apparatus (Perkin Elmer), was used with cooling and heating rates of $|dT/dt| = 10$ K/min in the temperature interval from 0°C down to −100°C, and annealing times of 5 min at $T = -100$°C. The TMDSC curve was recorded with sawtooth-like modulation and a frequency $\nu = \omega/2\pi = 16.7$ mHz. The amplitude of the first harmonic was 0.2 K, and the underlying cooling or heating rate was 0.5 K/min. The whole sample mass was about 30–40 mg, where the

mass fraction of BIBE in the pores amounts to 15–40% depending on the pore diameter. All samples were heated to 50°C for 5 min prior to any measurement.

3. Results

The DSC heating curves for BIBE in the porous glasses show a strong endothermic effect above the glass transition (Fig. 1) which is absent in the bulk liquid. This effect is especially pronounced for small pores or heating curves after fast cooling. We connect this effect with some kind of liquid structuring inside the pores and call it, correspondingly, 'structure peak'. Under such circumstances the estimation of reliable parameters for the step height and transition interval from DSC curves is not possible. This problem is also known for other liquids inside nanometer pores [20,21]. Cooling DSC curves are also not used because the high sample mass and thickness influence the shape of the measured curves to a great extent.

The TMDSC traces (Fig. 2) in cooling and heating mode, on the contrary, show in all cases the usual sigmoidal shape for the real part, $c_p'(T)$, with straight tangents above the dynamic glass transition. This demonstrates once more the different advantages of DSC and TMDSC techniques [22]. The imaginary part, $c_p''(T)$, in the heating mode shows some residual influence of liquid structuring depending on cooling history. But this remains well separated from the dynamic glass transition. TMDSC in cooling mode shows no such effects. The shapes of the glass transition peak in the imaginary part for cooling and heating mode are similar. Because the cooling mode starts with an equilibrium state those results were used.

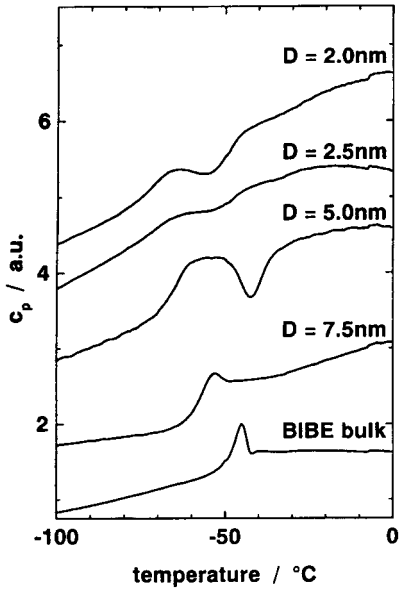

Fig. 1. DSC raw data for heating runs with 10 K/min after cooling with the same rate for BIBE as bulk material and within different pores of series I.

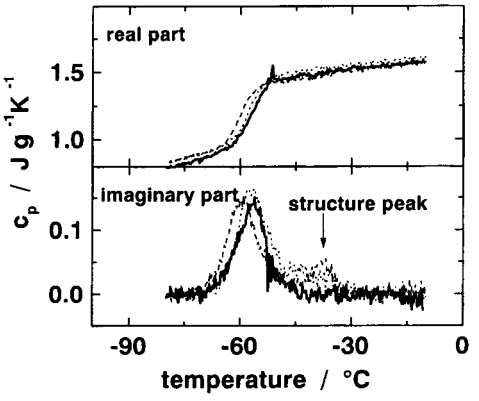

Fig. 2. Specific heat capacity of BIBE in the glass transition region from TMDSC. The bold line is for cooling mode. The thin lines are for heating mode after different cooling histories: dotted line for shock cooling and dashed line for cooling with 10 K/min from 50°C. For TMDSC parameters, see text.

The glass transition temperatures from TMDSC (taken at the maximum of the imaginary part $c_p''(T)$) for all samples are collected in Table 1. Also included are temperatures of maximum dielectric loss ε'' for the same measurement frequency $w = 2\pi \times 16.7$ mHz. Both values agree within experimental uncertainty. Slight differences between both values are expected [23] because they correspond to different activities, calorimetric and dielectric.

4. Discussion

Two points will be discussed: First the implications of the results for the picture of the hindered glass transition, and second the relation between the characteristic length ξ_α and the pore diameter D.

Table 1
Glass transition temperatures for BIBE at a frequency of ν=16.7 mHz from TMDSC (c_p'') and dielectrics (ε'')[a]

	Pore diameter							
	Bulk	7.5 nm		5 nm		2.5 nm		2 nm
		Series I	Series II	Series I	Series II	Series I	Series II	Series I
TMDSC	−50	−56	−52	−59	−53	−67	−55	−63
Dielectric	−49	−58	−50	−57	−52	−68	−57	−66

[a] All temperatures are from loss maxima (°C).

In the Adam–Gibbs model for cooperative relaxation [5] the curvature of the α relaxation trace in the Arrhenius diagram is intimately connected with an increasing cooperativity for decreasing temperature. If this growing spatial scale for a CRR reaches a limit induced by the geometric confinement no further increase is possible. Correspondingly, the trace of the relaxation in an Arrhenius diagram is expected to bend over from a WLF type into its tangent, i.e. to a simple activated Arrhenius behavior. This leads to smaller relaxation times (higher mobility) at low temperatures as compared to the extrapolated WLF trace. Correspondingly, the glass temperature decreases. This effect of increasing mobility inside nanometer pores was found by dielectric experiments for salol [24] and was termed hindered glass transition [12]. A corresponding picture of decreasing dynamic coupling within nanometer pores and the resulting decrease of glass transition temperature is also given in the framework of the coupling model [25]. If we assume an approximately constant characteristic length along the tangent in the Arrhenius diagram then the smaller value at the bend would be preserved. Calorimetry would then find smaller characteristic lengths even far below the bend temperature.

Fig. 3 shows the dependence of the glass transition temperature T_g, the width of the dispersion δT, the step height Δc_p, and the calorimetrically estimated characteristic length ξ_α (Eq. (1)) as a function of pore diameter D. Although the parameters of the two sample series are different the data for the characteristic length collapse on a single trace. This is a further argument in favour of this length.

Fig. 4 shows the correlation between the decreasing characteristic length ξ_α and the shift of the glass transition temperature to lower values. Although there are differences between the two sample series the general trend corresponds to the physical picture of the hindered glass transition.

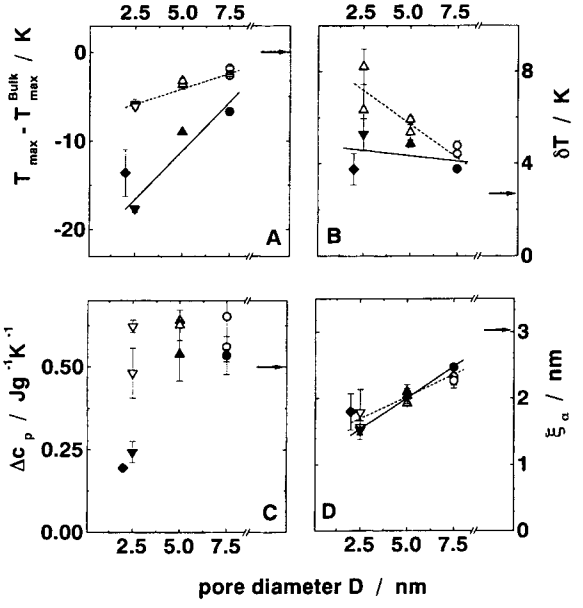

Fig. 3. Parameters for the dynamic glass transition estimated from the TMDSC traces as a function of the pore diameter D and for the bulk sample (indicated by arrows): (A) shift of the glass transition temperature compared to the bulk material; (B) the width of the dispersion δT; (C) the step height Δc_p; and (D) the characteristic length ξ_α. Solid symbols are for series I and open symbols for series II. Observe the collapse for both series for characteristic lengths in (D).

Let us now discuss the second point. Fig. 5 gives a detailed comparison of the different characteristic lengths as a function of pore diameter, $\xi_\alpha(D)$. This diagram is similar to Schick's used for the polymer poly(ethylene terephthalate) PET [1]. A limiting line $\xi_\alpha = D$ is given as the volume of one CRR $V_\alpha = \xi_\alpha^3$ is expected to remain smaller than the pore volume.

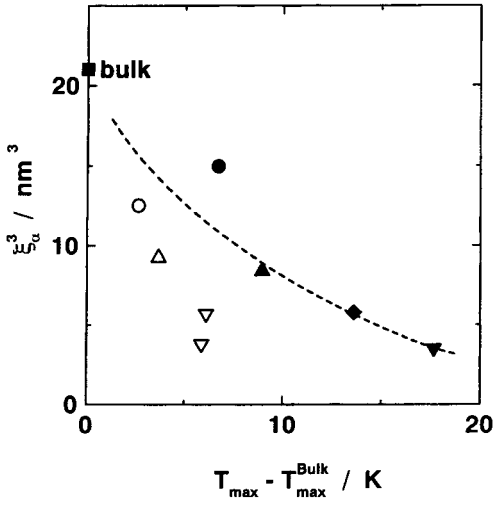

Fig. 4. Volume $V_\alpha = \xi_\alpha^3$ of a CRR inside the pores as a function of glass transition temperature depression (solid symbols for series I and open symbols for series II). The line for series I is only to guide the eye.

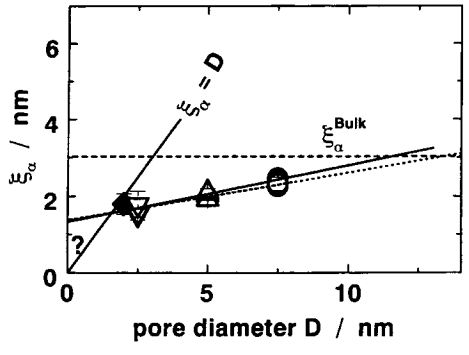

Fig. 5. Dependence of characteristic length ξ_α estimated from the calorimetric measurements (Eq. (1)) as a function of the pore diameter D. The characteristic length will be limited by ξ_α^{bulk} (dashed line) for big pores and perhaps by $\xi_\alpha = D$ for small ones, respectively. Solid and dotted line are linear fits for series I (solid symbols) and series II (open symbols), respectively.

The opposite is not impossible because the CRR may deform and connect different pores through the gates between them. The relation $\xi_\alpha = D$ was chosen as simplest case regarding the unknowns of pore geometry. No definite diameter–volume relation can be given. The thickness of the silanisized layer is also not exactly known and not included in the Fig. 5. If we subtract an appropriate amount from the pore diameter all data points would shift to the left.

The systematic decrease of the characteristic length ξ_α with decreasing pore diameter for both sample series corresponds to the physical picture of the hindered glass transition.

A linear regression for the values from both series enables extrapolations to the region of the first deviation from the bulk value at large D and to the limiting line $\xi_\alpha = D$ at small D. First deviations of the characteristic lengths ξ_α appear at pore diameters of 12–14 nm. This is far above the diameter of an individual CRR so that the bulk ξ_α cannot directly be determined from the geometric parameter D. For propylene glycol in porous glasses, and as droplets inside a network matrix, first effects on the dielectric α trace were also found for geometric confinements in the 12 nm region [8]. For OTP in porous glasses a decrease in T_g was found for pore diameters below 20 nm [20]. From measurements on thin polymeric films a strong decrease of glass temperature for films thicknesses below 80 nm was found [26]. This is of order the end-to-end distance of the polymer molecule, surely above the spatial scale responsible for the glass transition. Possibly, large scale deformations of the whole polymer molecule also change the more local conditions [25]. We speculate that the subtle condition of statistical independence [14] as used for the definition of a CRR is sensitive to external, confining influences even before the spatial restrictions reach the very dimensions of one CRR. This may also depend on dimensionality of the confinement [8]. For two-dimensional layers of mobile amorphous semicrystalline poly(ethylene terephthalate) the confinement is not so restrictive, and the deviation of the CRR size from bulk values occurs at only the twofold diameter of the bulk CRR [11]. For the more three-dimensional confinement as in our paper the deviation occurs at the fourfold to fivefold diameter of one bulk CRR.

The limiting line $\xi_\alpha = D$ is reached at a pore diameter of 1.6 nm. Unfortunately, no pores with diameters between 1 and 2 nm are available. Open questions are, if in this region the values of ξ_α follow the line $\xi_\alpha = D$ with a corresponding stronger decrease, if the trace of the α relaxation in the Arrhenius diagram reaches the trace of the local β relaxation, and if this relaxation remains calorimetrically active.

5. Conclusions

TMDSC enables the estimation of reliable parameters for the glass transition of molecular liquids inside nanometer pores not disturbed by effects of liquid structuring. The calorimetrically estimated characteristic length of the CRR ξ_α begins to deviate from the bulk value at pore diameters D around 12 nm. The length decreases from initially $\xi_\alpha = 3$ nm for the bulk material to $\xi_\alpha = 1.6$ nm for $D = 2.0$ nm. This is concomitant to a systematic decrease of the glass transition temperature. Both observations can be understood in the frame of the physical picture of a hindered glass transition. It remains an open question why the decrease begins for pore diameters so much above the size of an individual bulk CRR.

Acknowledgements

We thank the Deutsche Forschungsgemeinschaft DFG (Sonderforschungsbereich 418) and the Fonds der Chemischen Industrie FCI for financial support. Furthermore, we thank Dr. S. Zeeb for sample preparation.

References

[1] H. Sillescu, J. Non-Cryst. Solids 243 (1999) 81.
[2] K. Schmidt-Rohr, H.W. Spiess, Phys. Rev. Lett. 66 (1991) 3020.
[3] U. Tracht, M. Wilhelm, A. Heuer, H. Feng, K. Schmidt-Rohr, H.W. Spiess, Phys. Rev. Lett. 81 (1998) 2727.
[4] E. Donth, J. Non-Cryst. Solids 53 (1982) 325.
[5] G. Adam, J.H. Gibbs, J. Chem. Phys. 43 (1965) 139.
[6] R.L. Leheny, N. Menon, S.R. Nagel, D.L. Price, K. Suzuya, P. Thiyagarajan, J. Chem. Phys. 105 (1996) 7783.
[7] M. Arndt, R. Stannarius, H. Groothues, E. Hempel, F. Kremer, Phys. Rev. Lett. 79 (1997) 2077.
[8] P. Pissis, A. Kyritsis, G. Barut, R. Pelster, G. Nimtz, J. Non-Cryst. Solids 235 (1998) 444.
[9] A. Huwe, F. Kremer, P. Behrens, W. Schwieger, Phys. Rev. Lett. 82 (1999) 2338.
[10] J. Baschnagel, K. Binder, J. Phys. I (France) 6 (1996) 1271.
[11] C. Schick, E. Donth, Physica Scripta 43 (1991) 423.
[12] E. Donth, Glasübergang, Akademie, Berlin, 1981.
[13] E. Donth, J. Polym. Sci. B 34 (1996) 2881.
[14] E. Donth, Acta Polym. 50 (1999) 240.
[15] J. Korus, E. Hempel, M. Beiner, S. Kahle, E. Donth, Acta Polym. 48 (1997) 369.
[16] E. Hempel, G. Hempel, A. Hensel, C. Schick, E. Donth, to be published.
[17] S. Kahle, K. Schröter, E. Hempel, E. Donth, J. Chem. Phys., in press.
[18] S. Janowski, W. Heyer, Poröse Gläser, Herstellung, Eigenschaften und Anwendung, Deutscher Verlag für Grundstoffindustrie, Leipzig, 1982.
[19] D. Enke, Thesis, University Halle, 1998.
[20] C.L. Jackson, G.B. McKenna, Chem. Mater. 8 (1996) 2128.
[21] G.B. McKenna, Lecture at the EPS-Conference on Morphology and Micromechanics of Polymers, Merseburg, 27 September–1 October, 1998.
[22] B. Wunderlich, I. Okazaki, K. Ishikiriyama, A. Boller, Thermochim. Acta 324 (1998) 77.
[23] M. Beiner, J. Korus, H. Lockwenz, K. Schröter, E. Donth, Macromolecules 29 (1996) 5183.
[24] F. Kremer, A. Huwe, M. Arndt, P. Behrens, W. Schwieger, J. Phys.: Condens. Matt. 11 (1999) A175.
[25] K.L. Ngai, A.K. Rizos, D.J. Plazek, J. Non-Cryst. Solids 235 (1998) 435.
[26] J.A. Forrest, K. Dalnoki-Veress, J.R. Dutcher, Phys. Rev. E 56 (1997) 5705.